Proceedings of the 4th International Conference on Functional Materials and Civil Engineering
DOI: 10.54254/2755-2721/2026.38025

First-Principles Study of Band-Gap Evolution in Monolayer MoS_2 under Biaxial Strain

Yixiu Wu

School of Materials Science and Engineering, Central South University, Changsha, China
2596701604@qq.com

Abstract. Two-dimensional transition-metal dichalcogenides have become important candidate materials for post-silicon semiconductors and optoelectronic devices because of their atomic-scale thickness, tunable band gaps, and good device compatibility. The electronic structure of monolayer MoS_2 is highly sensitive to strain. In-plane biaxial strain can continuously tune both the magnitude and the direct/indirect character of the band gap by changing Mo–S bond lengths and orbital hybridization. Based on density-functional theory, this work systematically performs first-principles calculations on the electronic structure of monolayer 1H-MoS_2 under biaxial strains from −6% to +8% in Quantum ESPRESSO, using the PBE functional and PAW pseudopotentials. At each strain point, ionic relaxation, self-consistent field calculation, and Γ–K–M–Γ band analysis are completed, and the fundamental gap, the K–K direct gap, and the Γ–K indirect gap are extracted simultaneously. The results show that under −2% compressive strain the system exhibits a K–K direct gap with a fundamental gap of 1.890 eV; near zero strain the K–K and Γ–K gaps are nearly degenerate (1.686 eV and 1.667 eV, respectively); after entering the tensile regime, the valence-band maximum shifts to Γ while the conduction-band minimum remains at K, forming a stable indirect gap, and the fundamental gap decreases monotonically from 1.667 eV at 0% to 0.589 eV at +8%. Gaps on the compressive side remain overall larger and reach a maximum of 1.919 eV at −4% within the present scan. This study provides a reproducible strain–band-gap relation and transition criterion, and offers a benchmark for band-gap engineering of two-dimensional MoS_2 and for subsequent higher-accuracy calculations.

Keywords: monolayer MoS_2, biaxial strain, band-gap engineering, first principles, Quantum ESPRESSO

1. Introduction

The emergence of two-dimensional materials has expanded the boundaries of semiconductor physics and device design. Unlike gapless graphene, monolayer transition-metal dichalcogenides (TMDs) possess finite and tunable band gaps. Among them, MoS_2 has received sustained attention because of its relatively mature fabrication processes, optical response in the visible range, and potential for field-effect devices [1-3]. Experimental and theoretical studies show that when MoS_2 is thinned from the bulk to the monolayer limit, its band gap can change from indirect to direct and the

© 2026 The Authors. This is an open access article distributed under the terms of the Creative Commons Attribution License 4.0 (https://creativecommons.org/licenses/by/4.0/).

DOI: 10.54254/2755-2721/2026.38025

luminescence efficiency increases significantly [1, 2]. Furthermore, in-plane strain, substrate coupling, dielectric environment, and external fields can all rearrange band edges, thereby tuning carrier effective masses, optical absorption onsets, and valleytronic properties [4-6].

Among various tuning approaches, strain engineering is continuous, reversible, and compatible with flexible electronics. Biaxial strain simultaneously changes the in-plane lattice constant, directly modulates Mo–S bond lengths and the strength of d–p orbital hybridization, and thereby shifts the relative positions of the valence-band maximum (VBM) and the conduction-band minimum (CBM) [5-8]. Existing first-principles studies indicate that tensile strain usually reduces the monolayer MoS_2 band gap and induces a direct-to-indirect transition, whereas compressive strain tends to enlarge or maintain a larger gap [6-8]. In recent years, research on strain-based band-gap engineering of two-dimensional materials has continued to advance, indicating that this direction remains practically relevant for device design [9-12].

Using Quantum ESPRESSO as the computational platform, this paper addresses the following questions: (1) How does biaxial strain quantitatively change the fundamental gap of monolayer MoS_2? (2) In which strain range does the direct–indirect band-gap transition occur? (3) How are the VBM and CBM reordered with strain among high-symmetry points such as Γ and K? The significance of this study is twofold: it provides a reproducible PBE-level strain–band-gap relation, and it clarifies the sensitivity of gap type near zero strain, thereby offering a benchmark for subsequent higher-accuracy calculations and experimental comparison.

2. Computational model and methods

2.1. Structural model

A monolayer 1H-MoS_2 primitive cell is adopted, containing one Mo atom and two S atoms. The initial in-plane lattice constant is taken as a_0 = 3.18 Å, and a vacuum thickness of 20 Å is used to suppress spurious interlayer periodic-image interactions. The upper and lower sulfur atoms are aligned in the in-plane projection and located on opposite sides of the Mo plane, corresponding to the 1H phase rather than the 1T phase. Biaxial strain is defined as $\varepsilon = (a - a_0)/a_0 \times 100\%$. The strain points scanned in this work are $\varepsilon = -6\%, -4\%, -2\%, 0, +2\%, +4\%, +6\%$, and $+8\%$. At each strain point, the in-plane lattice constant is fixed and only the internal atomic coordinates are relaxed.

2.2. First-principles calculations

All calculations are performed in Quantum ESPRESSO [13]. The exchange-correlation functional is PBE [14], and PAW-type PBE pseudopotentials are used: Mo.pbe-spn-kjpaw_psl.1.0.0.UPF and S.pbe-n-kjpaw_psl.1.0.0.UPF. The total number of valence electrons is 26, and the number of occupied bands in non-spin-polarized calculations is 13. The main results in the main text adopt the production settings: ecutwfc = 50 Ry and ecutrho = 400 Ry; 9×9×1 and 12×12×1 Monkhorst–Pack k-point meshes are used for structural relaxation and self-consistent calculations, respectively. An additional rapid scan with ecutwfc = 30 Ry and k = 6×6×1 is performed for cross-validation. The band path is Γ–K–M–Γ.

The computational workflow is as follows: (1) ionic relaxation at fixed lattice constants (BFGS); (2) self-consistent field (SCF) calculation; (3) non-self-consistent band-structure calculation; and (4) extraction of the VBM, CBM, fundamental gap, and local gaps at high-symmetry points from the band data. In determining the gap type, the K–K direct gap and the Γ–K indirect gap are compared

DOI: 10.54254/2755-2721/2026.38025

simultaneously. If both the VBM and the CBM lie near the K point, the gap is recorded as direct; if the VBM lies at Γ and the CBM at K, the gap is recorded as indirect.

2.3. Definition of analyzed quantities

To avoid misjudgment caused by relying only on global extrema, this work reports simultaneously the fundamental gap E_g, the K-point direct gap E_g(K–K), the Γ–K indirect gap E_g(Γ–K), and ΔE_VBM = E_VBM(K) − E_VBM(Γ). When ΔE_VBM > 0, the VBM prefers K; when ΔE_VBM < 0, the VBM prefers Γ.

3. Results and discussion

3.1. Zero-strain reference

Under the production settings, the fundamental gap of unstrained monolayer MoS_2 is 1.667 eV, with the VBM at Γ and the CBM at K, corresponding to a Γ–K indirect gap. At the same time, the K–K direct gap is 1.686 eV, only about 0.019 eV higher than the fundamental gap. In other words, the direct and indirect gaps are nearly degenerate near zero strain. The rapid scan yields an unstrained fundamental gap of 1.666 eV, in close agreement with the production result, indicating that the subsequent strain-trend analysis is robust with respect to the computational parameters.

It should be noted that the experimental optical gap of monolayer MoS_2 is usually larger, and PBE systematically underestimates band gaps. In addition, whether a direct gap appears depends strongly on the equilibrium lattice constant, spin-orbit coupling (SOC), and k-point sampling. In this work, a_0 is fixed at 3.18 Å and SOC is not included at this stage; therefore, the zero-strain result should be understood as a PBE-level electronic-structure reference at the chosen lattice constant, rather than an exact reproduction of the experimental direct gap.

3.2. Overall evolution of the band gap under biaxial strain

The full set of production-parameter results shows that the band gap of monolayer MoS_2 is highly sensitive to strain. The main data are summarized in Table 1, and the corresponding strain dependence is shown in Figure 1. From 0 to +8%, the fundamental gap decreases from 1.667 eV to 0.589 eV, corresponding to an average reduction of about 0.13 eV per 1% tensile strain. This "tensile strain reduces the gap" trend is consistent with existing strain-engineering studies of two-dimensional MoS_2 [6-11]. Gaps on the compressive side remain overall larger than the unstrained value and reach a maximum of 1.919 eV near −4% within the scanned range.

Table 1. Band gaps and gap types under different biaxial strains (production settings, PBE)

Strain/%	Eg/eV	K–K/eV	Γ–K/eV	ΔEVBM	Type
-6	1.880	2.379	2.926	+0.547	Large gap
-4	1.919	2.121	2.459	+0.339	Large gap
-2	1.890	1.890	2.040	+0.150	Direct K–K
0	1.667	1.686	1.667	-0.019	Near-deg.
+2	1.338	1.508	1.338	-0.169	Indirect Γ–K
+4	1.051	1.353	1.051	-0.302	Indirect Γ–K

DOI: 10.54254/2755-2721/2026.38025

Table 1. (continued)

+6	0.802	1.220	0.802	-0.417	Indirect Γ–K
+8	0.589	1.105	0.589	-0.516	Indirect Γ–K

3.3. Direct–indirect band-gap transition

The change in gap type is the central phenomenon of this work. Data analysis shows that under moderate compressive strain (about −2%), both the VBM and the CBM lie at K, the system is a direct-gap semiconductor, and E_g(K–K) = 1.890 eV. Near zero strain, E_VBM(K) and E_VBM(Γ) are nearly equal (ΔE_VBM = −0.019 eV), so the ground state can switch between K–K and Γ–K and belongs to a near-transition point. Under tensile strain (≥ +2%), the VBM clearly shifts to Γ while the CBM remains at K, forming a stable Γ–K indirect gap, and the indirect character becomes more pronounced with increasing tensile strain. The evolution of the VBM and CBM with strain is summarized in Figure 2.

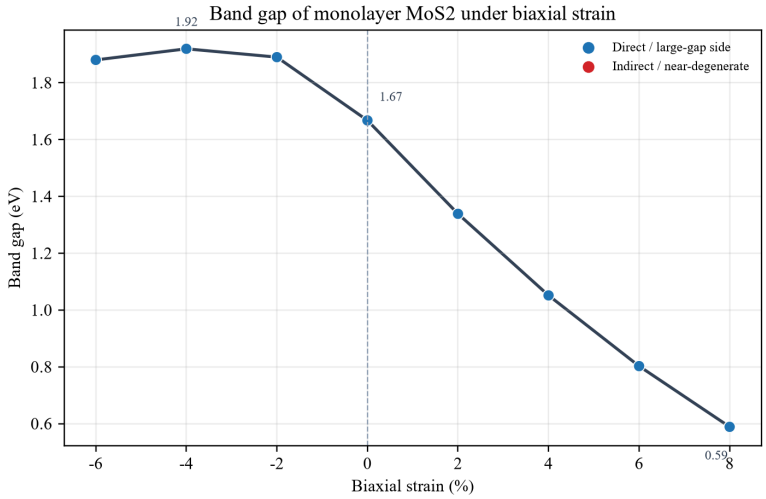

Figure 1. Band gap versus biaxial strain

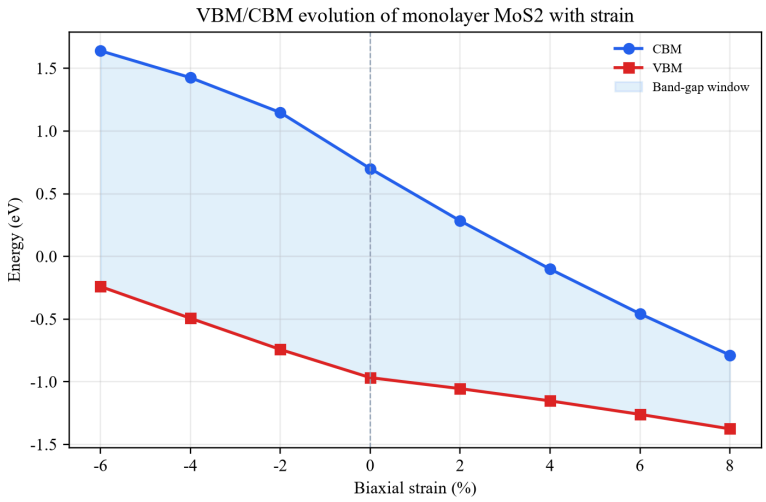

Figure 2. Evolution of VBM/CBM with strain

DOI: 10.54254/2755-2721/2026.38025

From an orbital and bonding viewpoint, tensile strain elongates Mo–S bonds and weakens in-plane coupling, relatively raising Γ-related valence-band states (or relatively lowering the K valence band), thereby changing the VBM ordering; at the same time, the K-point conduction-band state continues to descend, leading to gap reduction. Compressive strain strengthens orbital overlap, raises conduction-related states, and stabilizes the K-point valence-band advantage, favoring the coexistence of a direct gap and a larger gap. For −4% and −6%, the global CBM does not sit exactly at K but appears near the Γ–K path, indicating that under strong compression the conduction-band minimum may shift along the line path. This point can be further confirmed later with denser k paths or a full Brillouin-zone extremum search.

3.4. Representative band-structure comparison

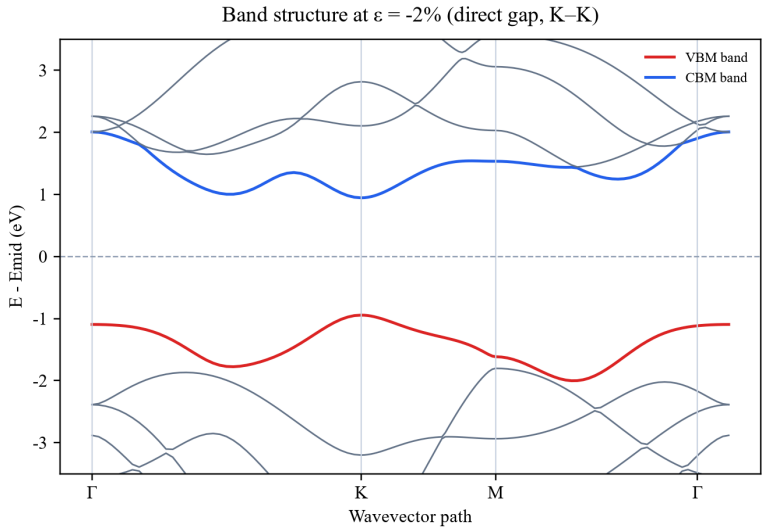

Figure 3. ε = −2% (direct gap, K–K)

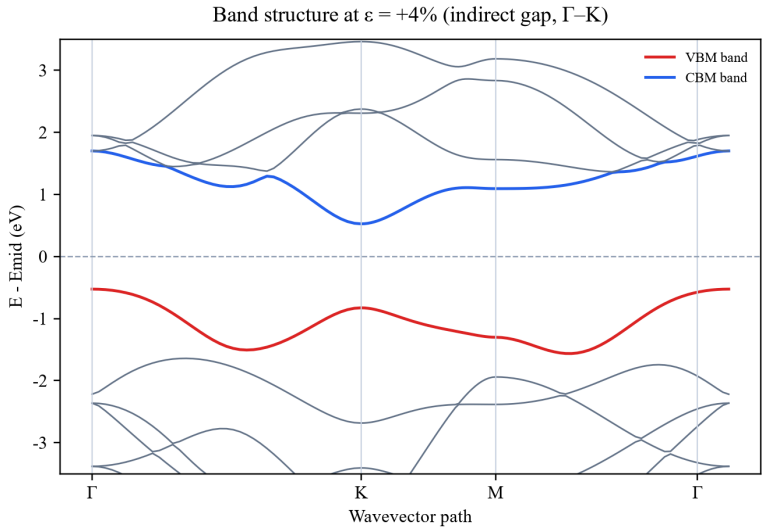

Figure 4. ε = +4% (indirect gap, Γ–K)

DOI: 10.54254/2755-2721/2026.38025

Comparison of the representative band structures at −2% and +4% (Figures 3 and 4) reveals a clear physical picture: at −2%, a sharp direct-transition channel forms at K, and the valence band at Γ lies below that at K; after entering +4%, the Γ valence-band maximum is significantly higher than K, while the conduction-band minimum deepens at K, giving a clear indirect-gap character. Complete band structures for near-degeneracy at zero strain and further gap reduction at +8% are available in the results directory.

Supplementary comparison shows that at $\varepsilon = 0$ the Γ/K valence bands are nearly degenerate, while at $\varepsilon = +8\%$ the indirect gap further shrinks to 0.589 eV (the complete set of four band-structure figures is available in the results directory).

This implies that if the target is a light-emitting device, one should preferably operate under slight compression or near-zero strain and ensure that the K–K channel dominates; if the goal is to lower the optical absorption edge by strain or to tune the relative positions of dark and bright states, tensile strain can be used to enter the indirect-gap regime. Of course, because absolute PBE gaps are low, quantitative device design still requires HSE06 or GW-level corrections [15, 16].

4. Conclusions

Based on Quantum ESPRESSO and the PBE functional, this work has completed first-principles band-structure calculations for monolayer 1H-MoS_2 under biaxial strains from −6% to +8%. The main conclusions are as follows.

First, biaxial strain is an efficient means of tuning the band gap of monolayer MoS_2. Tensile strain reduces the fundamental gap in an approximately linear manner, from 1.667 eV at 0% to 0.589 eV at +8%; compressive strain keeps the gap at a higher level and reaches 1.919 eV near −4%.

Second, the gap type evolves markedly with strain. Around −2%, the system exhibits a K–K direct gap; near zero strain the K–K and Γ–K gaps are nearly degenerate; after entering the tensile regime, the VBM shifts to Γ and the CBM remains at K, forming a stable indirect gap. This transition can be directly characterized by the sign change of $\Delta E_VBM = E_VBM(K) - E_VBM(\Gamma)$.

Third, for the three questions raised in the Introduction, the answers are as follows: the gap decreases significantly under tensile strain and increases under compressive strain; the direct/indirect transition occurs in a narrow window near zero strain; and the microscopic mechanism is the reordering of the Γ and K valence bands together with the continued descent of the K-point conduction band.

This study still has limitations. First, PBE underestimates the band gap, so absolute values should not be matched one-to-one with optical experiments. Second, systematic variable-cell relaxation has not yet been performed to determine the PBE equilibrium a_0, and SOC has not been included. Third, the precise location of the CBM under strong compression still needs confirmation with denser k paths. Future work may proceed along three routes: first perform vc-relax and convergence tests for the unstrained system; then introduce SOC to discuss valley splitting and transition matrix elements; and finally correct absolute gap values with HSE06/GW and compare with micro-photoluminescence, strain Raman, and other experiments. Overall, this work demonstrates that the logical chain "strain–bond length–orbital hybridization–band ordering–gap type" holds clearly in monolayer MoS_2 and can provide a computational basis for band-gap engineering of two-dimensional semiconductors.

DOI: 10.54254/2755-2721/2026.38025

References

[1] Mak, K. F., Lee, C., Hone, J., Shan, J., & Heinz, T. F. (2010). Atomically thin MoS_2: A new direct-gap semiconductor. *Physical Review Letters, 105*(13), 136805. DOI: 10.1103/PhysRevLett.105.136805.

[2] Splendiani, A., et al. (2010). Emerging photoluminescence in monolayer MoS_2. *Nano Letters, 10*(4), 1271–1275. DOI: 10.1021/nl903868w.

[3] Radisavljevic, B., Radenovic, A., Brivio, J., Giacometti, V., & Kis, A. (2011). Single-layer MoS_2 transistors. *Nature Nanotechnology, 6*, 147–150. DOI: 10.1038/nnano.2010.279.

[4] Wang, Q. H., Kalantar-Zadeh, K., Kis, A., Coleman, J. N., & Strano, M. S. (2012). Electronics and optoelectronics of two-dimensional transition metal dichalcogenides. *Nature Nanotechnology, 7*, 699–712. DOI: 10.1038/nnano.2012.193.

[5] Conley, H. J., et al. (2013). Bandgap engineering of strained monolayer and bilayer MoS_2. *Nano Letters, 13*(8), 3626–3630. DOI: 10.1021/nl4014748.

[6] Johari, P., & Shenoy, V. B. (2012). Tuning the electronic properties of semiconducting transition metal dichalcogenides by applying mechanical strains. *ACS Nano, 6*(6), 5449–5456. DOI: 10.1021/nn301320r.

[7] Peelaers, H., & Van de Walle, C. G. (2012). Effects of strain on band structure and effective masses in MoS_2. *Physical Review B, 86*(24), 241401. DOI: 10.1103/PhysRevB.86.241401.

[8] Lloyd, D., et al. (2016). Band gap engineering with ultralarge biaxial strains in suspended monolayer MoS_2. *Nano Letters, 16*(9), 5836–5841. DOI: 10.1021/acs.nanolett.6b02615.

[9] Wang, C., Li, S., Wang, S., et al. (2023). Effect of biaxial [110] strain on monolayer MoS_2 and its vacancy defect system: A first-principles study. *Journal of Solid State Chemistry, 317*, 123711. DOI: 10.1016/j.jssc.2022.123711.

[10] Sah, R. K., Tang, H., Shahi, C., Ruzsinszky, A., & Perdew, J. P. (2024). Effect of strain on the band gap of monolayer MoS_2. *Physical Review B, 110*(14), 144109. DOI: 10.1103/PhysRevB.110.144109.

[11] Javed, A., Asif, M., & Ullah, R. (2024). Band gap crossover and symmetry breaking in strained monolayer MoS_2. *Materials Letters, 372*, 137066. DOI: 10.1016/j.matlet.2024.137066.

[12] Wei, R., Liu, G., Gao, X., et al. (2023). Effect of strain on the electronic structure and optical properties of Cr-doped monolayer MoS_2. *Journal of Molecular Modeling, 29*(11), 331. DOI: 10.1007/s00894-023-05735-w.

[13] Giannozzi, P., et al. (2009). Quantum ESPRESSO: A modular and open-source software project for quantum simulations of materials. *Journal of Physics: Condensed Matter, 21*(39), 395502. https://doi.org/10.1088/0953-8984/21/39/395502

[14] Perdew, J. P., Burke, K., & Ernzerhof, M. (1996). Generalized gradient approximation made simple. *Physical Review Letters, 77*(18), 3865–3868. https://doi.org/10.1103/PhysRevLett.77.3865

[15] Heyd, J., Scuseria, G. E., & Ernzerhof, M. (2003). Hybrid functionals based on a screened Coulomb potential. *The Journal of Chemical Physics, 118*(18), 8207–8215. https://doi.org/10.1063/1.1564060

[16] Hybertsen, M. S., & Louie, S. G. (1986). Electron correlation in semiconductors and insulators: Band gaps and quasiparticle energies. *Physical Review B, 34*(8), 5390–5413. https://doi.org/10.1103/PhysRevB.34.5390